16TH EUROPEAN CONFERENCE ON EARTHQUAKE ENGINEERING THESSALONIKI 18 - 21 JUNE 2018

DEVELOPMENT OF RESILIENT REINFORCED CONCRETE BUILDING STRUCTURAL SYSTEM

Susumu Kono[1], Ryo Kuwabara[2], Fuhito Kitamura[2], Eko Yuniarsyah[2], Hidekazu Watanabe[3], Tomohisa Mukai[3], and David Mukai[4]

ABSTRACT

Two real scale five-story reinforced concrete frame buildings were tested in BRI in order to evaluate damage of reinforced concrete structural members such as beams, columns and walls for strength-based design buildings. A series of experimental works show that secondary RC walls could have improved seismic performance for damage reduction by changing configuration and rebar arrangement. This strength enhancement with ductile detailing is one of the easiest and most economical solutions to reduce seismic damage. The paper describes current research efforts on resilient reinforced concrete structures in Japan focusing on complete residual flexural crack profile simulation (crack spacing, width, and length). Numerical procedures using FEM analysis are introduced and the computed results are compared to the real scale experimental results. The information will be helpful to evaluate cost of repair after earthquake damage.

Keywords: Resilient buildings; low damage structural system; quick recovery; damage evaluation from cracking and crushing

1. INTRODUCTION

Damage to non-structural (or secondary) members are as important as that to structural members from the view point of continuous post-earthquake functionality. Resilience of building structures specifically means low or no damage of structural and non-structural (or secondary) members and quick recovery of functions of buildings. In order to achieve resilient building structures, it is important to develop low damage structural systems in a broader sense and propose design procedures to advance the idea.

Engineers in National Institute for Land and Infrastructure Management (NILIM) and Building Research Institute (BRI) designed and tested real scale five story reinforced concrete buildings to see seismic performance of strength-based building system. Three universities and seven companies joined the experimental works at BRI to closely observe damage at different loading stages. The building introduced in this paper was tested in 2014 (Kabeyasawa et al. 2016 and 2017). The designed concrete frame building had higher load carrying capacity by adding wing walls to columns, or standing or/and hanging walls to beams. It was supposed to possess load carrying capacity equivalent to C_0=0.45 - 0.55 (C_0: base shear coefficient) at mechanism formation with maximum interstory drift as small as 0.4% - 0.8%. This implies that the building would have an elastic or nearly elastic response even under large scale earthquakes. Limited deformation would result in dramatic damage reduction in columns, beams, and beam-column connections. This paper discusses features of cracks from a numerical view point. A crack simulation procedure is introduced by revising the former strain based concept (Kono et al. 2017).

[1]Professor, Inst. of Innovative Research, Tokyo Inst. of Technology, Japan, kono.s.ae@m.titech.ac.jp
[2]Graduate Student, Tokyo Inst. of Technology, Japan
[3]Research fellow, Building Research Institute, Japan, wata_h@kenken.go.jp, t_mukai@kenken.go.jp
[4]Associate Professor, Univ. of Wyoming, (Visiting Assoc. Prof., Tokyo Inst. of Tech.), dmukai@uwyo.edu

2. EXPERIMENTAL WORK

Figure 1 shows configuration of a five-story RC specimen and typical section size with reinforcement arrangement. It is noted that the building had structural slits (or gaps) between secondary walls as shown by thick blue lines in Figure 1(a). Cracks were traced and copied to transparencies and the maximum width for each crack was recorded (Figure 2).

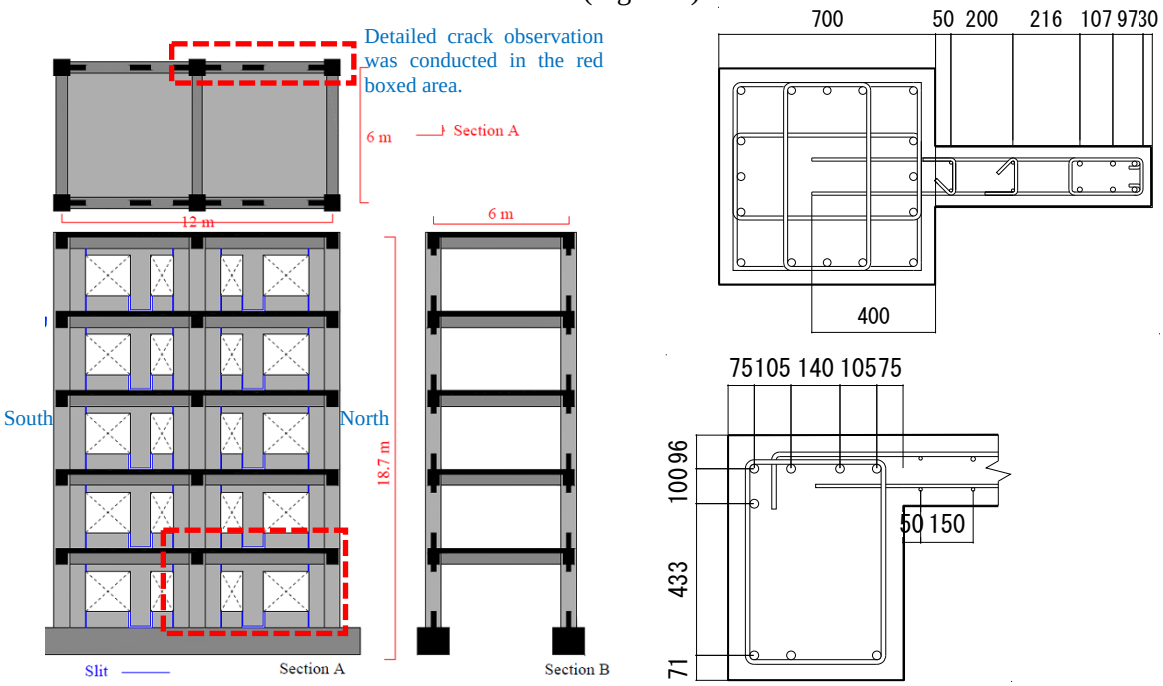

(a) Specimen configuration (b) Column with a wing wall and beam with one side slab

Figure 1. Configuration of the 2014 five story specimen and typical section size (Fukuyama et al. 2015)

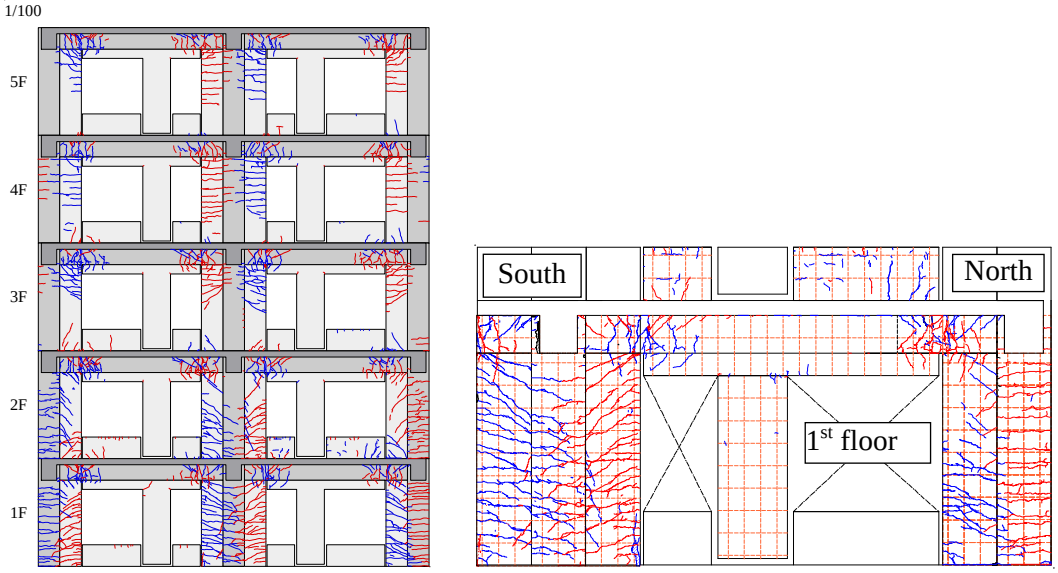

(a) Overall view (Kabeyasawa et al. 2016) (b) Area for detailed observation (Kitamura 2017)

Figure 2. Recorded cracks and spalling at R=1%

3. SIMULATION OF FLEXURAL CRACKS

A procedure to evaluate residual cracks are introduced in Figure 3. Based on numerical FEM analysis, it is aimed to obtain complete residual flexural crack profiles (crack spacing, width, and length). The flow has two branches in the midway; flow for residual flexural crack width and flow for crack length. Blue boxes (#3 and #7) are predetermined values and red boxes (#5 and #9) are values obtained from a regression analysis. Crack spacing (#3) is determined based on CEB-FIP Model Code equation (1978) although it is not necessarily for seismic purposes. Residual flexural crack width (#6) is obtained from the peak flexural crack width (#4). Conversion from peak to residual values is conducted by multiplying factor, γ (#5), which is obtained from a regression analysis. Horizontal crack length, L_h, is counted (#8) when crack width is larger than visible flexural crack width W_{limit} =0.01mm (#7). Then actual diagonal and meandering crack length (#10), L_f, is obtained by multiplying correction factor (#9), α, which is also obtained from a regression analysis. From #3, #6, and #10, complete residual flexural crack profiles (spacing, width, and length) are obtained.

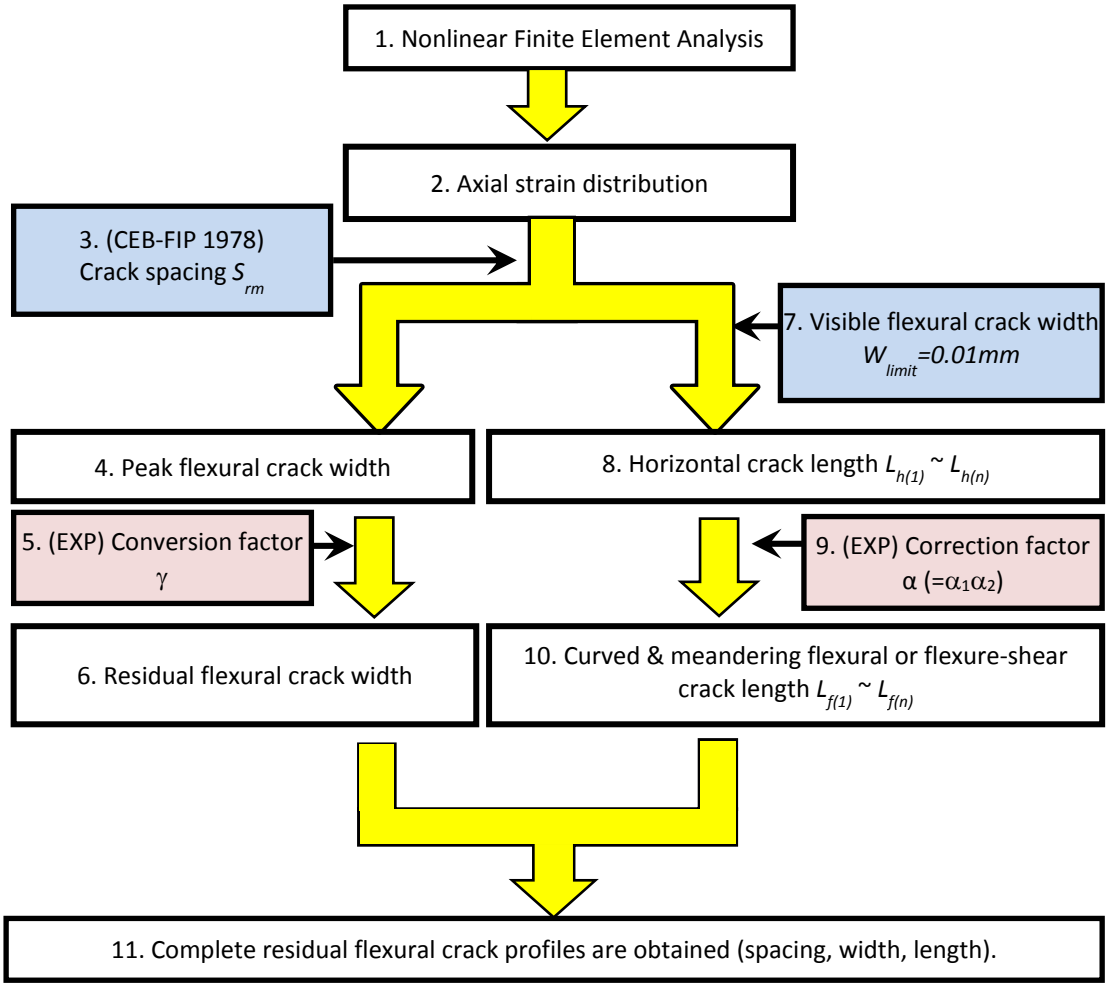

Figure 3. Flow chart how to obtain complete residual flexural crack profiles

3.1 Numerical analysis with an FEM program

Figure 4 shows a 2D finite element mesh used in a commercial FEM program "FINAL" (ITOCHU 2016). Concrete was modeled as isoparametric quadrilateral elements with smeared reinforcement, and longitudinal reinforcement was modeled as beam-column elements. Perfect bond characteristics were assumed for all reinforcement. All degrees of freedom were fixed at nodes on the bottom face of the foundation beams. Self-weight was applied as concentrated load at beam-column connections based on a tributary area. Lateral load was applied at the central beam-column connections of roof and fourth floor by 1:2 ratio to simulate the load conditions in experiment. Load was controlled by the lateral displacement of the roof level and loading protocol followed the measured displacement although the second cycle was skipped to save computational time. The numerical simulation was carried out up to R=1% since the resisting mechanism of building changed when structural slits (or gaps) closed at R=1.3% in experiment. The elements employed default material models; modified Ahmad model (Naganuma 1995) and Izumo model (Izumo et al. 1987) were used for concrete and modified Menegotto-Pinto model (Ciampi et al. 1982) was used for reinforcement.

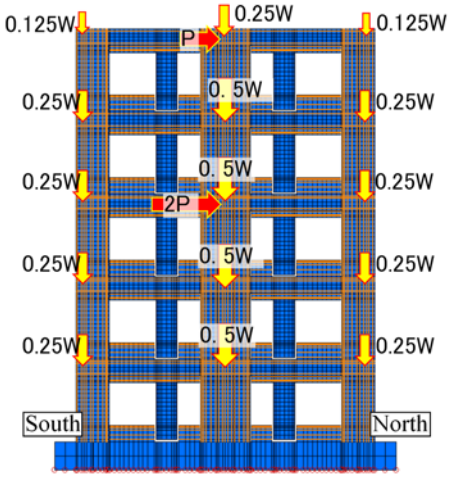

Figure 4. Finite element mesh and loading condition in *2D* finite element analysis (Kitamura 2017)

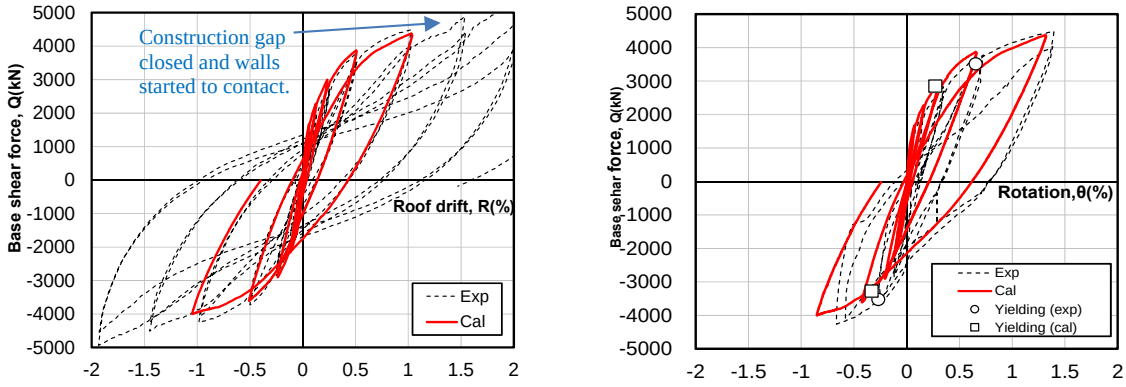

(a) Base shear force – roof level drift ratio relation (b) Base shear – 1F north column rotation angle

Figure 5. Typical results of finite element analysis (Kitamura 2017)

Figure 5(a) shows base shear force – roof level drift relation. The numerical simulation agrees well with the experimental results. Figure 5(b) shows the base shear force – member rotation of the north column (1F). The deformation of each member directly influences the simulation of crack performance. The simulated curve agreed relatively well with the experimental results in the positive side but did not agree very well in the negative side. The results for the beam (2F) and wing wall (1F) had similar trend although their plots are not shown.

3.2 Numerical simulation of flexural cracks

Most cracks were governed by flexure as can be seen in Figure 2 and numerical simulation in this paper treated only flexural cracks. An effect of some flexural-shear cracks was considered with conversion index, α, which is explained later. Treatment of shear cracking is also important but will be discussed elsewhere. The first floor column is used as an example to explain how to obtain spacing, width, and length of flexural cracks.

First, the left flow (#3, 4, 5, and 6) in Figure 3 is explained step by step. Crack width, W_i, was computed based on Eq. (1). It was assumed that concrete does not deform and elongation of a member comes from crack openings. Hence, strain obtained from the finite element analysis represents effects of smeared cracks. Based on this assumption, the flexural crack width of a member can be obtained by integrating longitudinal tensile strain (ε_{zz}) over a crack spacing (s_{rm}). The crack spacing is based on Eq. (2) proposed in CEB-FIP Model Code (CEB-FIP 1978). Equation (2) is based on the condition that the number of cracks reached saturated condition. The error of the equation was studied beforehand and turned out to be reasonably small after R=0.25%.

$$W_i = \int_{h_i - s_{rm}/2}^{h_i + s_{rm}/2} \varepsilon_{zz}\, dz \tag{1}$$

$$s_{rm} = 2\left(c_s + \frac{s_y}{10}\right) + k_1 k_2 \frac{d_{by}}{p_y} \tag{2}$$

where W_i and h_i are crack width and height of the i-th crack, ε_{zz} is tensile strain in vertical (z) direction, s_{rm} is crack spacing. Other notations in Eq. (2) should be referred to the original document. Figure 6 shows accumulated crack width for the north column (1F) and the wing wall (1F). Crack width was accumulated from the top to bottom. The accumulated crack width at the bottom is close to the elongation measured by displacement gages, and measured elongation of member is expressed by the vertical break lines in the figure. Figure 6(a) and (c) shows variaions at the peaks and Figure 6(b) and (d) show those at the unloaded conditions. Each figure has comparisons between experimental and anlytical results for three drift levels at R=0.25%, 0.5% and 1%. Residual crack width was obtained by multiplying reduction factor, γ, which was determined from regression analysis of test results for each type of member. Solid circles on the expecimental curves show the location of actural cracks and those for analysis show simulated points with spacing, s_{rm}. Simulated variations for peak load agreed relatively well with experimental rusults for the column and wing wall. However, the agreement is not very good for residual crack width. If the total elongation of the tension fiber in analysis does not agree with exerimental results, the simulation does not agree with the experimental resutls. Although the AIJ guidelines (AIJ 2004) assumes that residual crack width is half of the peak crack width regardless of axial load mainly to achieve simplicity and conservatism, this concept should be revised based on expremental results.

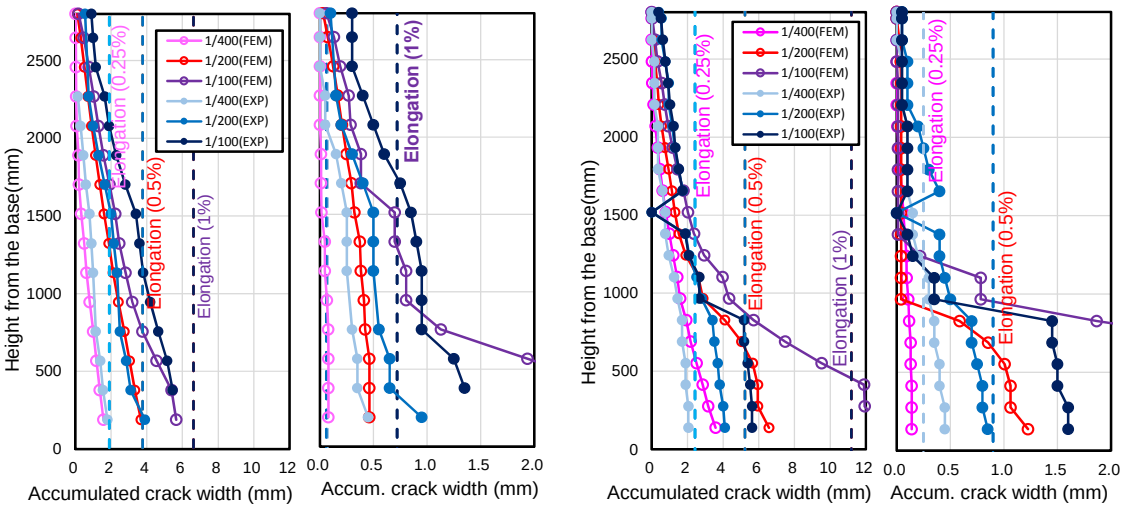

(a) North column (peak) (b) North column (residual) (c) North Wing wall (peak) (b) North Wing wall (residual)
Figure 6. Accumulated crack width distribution

Secondly, the right flow (#7, 8, 9, and 10) in Figure 3 is explained. Crack length was computed using analytical results of FEM as well. The crack is assumed visible when crack width of the *i*-th crack exceeds the limit crack width, W_{limit}, which is a constant value and defined in Eq. (3). The projectected crack length, $L_{h(i)}$,was computed based on the neutral axis depth, $x_{n(i)}$, and invisible crack length, $x_{limit(i)}$, as shown in Eq. (4) and Figure 7. In this paper, the crack opening profile is assumed triangular as shown in Figure 7(d) and the computing process is based on the edge opening, W_i.

$$W_{limit} = 0.01\text{mm} \text{ in this study} \tag{3}$$

$$L_{h(i)} = D - x_{n(i)} - x_{limit(i)} \tag{4}$$

$$L_{f(i)} = \alpha L_{h(i)} \tag{5}$$

$$\alpha = \alpha_1 \cdot \alpha_2 \tag{6}$$

$$\alpha_1 = average\left(\frac{L_{f(exp)}}{L_{d(exp)}}\right) \text{ (from straight length to meandering length)} \tag{7}$$

$$\alpha_2 = average\left(\frac{L_{d(exp)}}{L_{h(exp)}}\right) \text{ (from horizontal projection to diagonal length)} \tag{8}$$

Conversion index, α, was multiplied to obtain actural diagonal and meandering crack length, $L_{f(i)}$, to take into account the fact that cracks are not smooth nor horizontal. Index, α, was determined from the experimetal results and the values were 1.15, 1.28, and 1.51 for the column, wing wall, and beam. Index α_1 and α_2 were computed using regression analysis of experimental data using Eqs. (7) and (8).

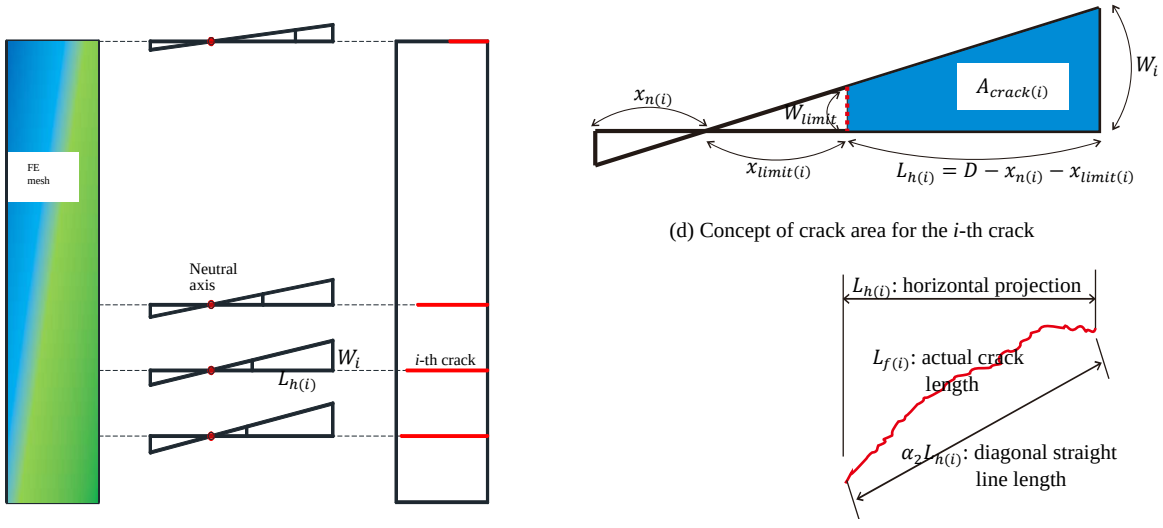

(a) Strain (ε_{zz}) contour (b) Location of neutral axis (c) horizontal crack length

(d) Concept of crack area for the *i*-th crack

(e) Conversion to an actual meandering crack

Figure 7. Calculation of crack length

Since complete profiles of residual flexural crack profiles have been obtained (Crack spacing in #3, residual crack width in #6, and crack length in #10 in Figure 3), they are validated with experimental data. Figure 8 shows crack area damage ratio, β_A, which is the ratio of all visible crack area summation, $\sum A_{crack(i)}$, to the concrete surface area, $A_{surface}$. It is a no-dimensional quantity as expressed by Eq. (9). Crack area is defined in Figure 7(d) as a blue trapezoid shape.

$$\beta_A = \frac{\sum A_{crack(i)}}{A_{surface}} = \frac{\sum\{0.5 \cdot W_i \cdot (D - x_{n(i)}) - 0.5 \cdot W_{limit} \cdot x_{limit(i)}\}}{A_{surface}} \tag{9}$$

where D is the total depth of a member. Based on the reference (JBDPA 2015), crack width is categorized into four classes of crack width ($0 \leq w_{cr} \leq 0.2mm$, $0.2mm \leq w_{cr} \leq 1mm$, $1\text{mm} \leq w_{cr} \leq 2mm$ $w_{cr} \geq 2mm$) and β_A for each category is expressed as a stack graph in Figure 8. Envelop curve is simulated relatively well for the column. Although it is not shown, the simulation is not very good for wall and beam because the crack width simulation did not work well.

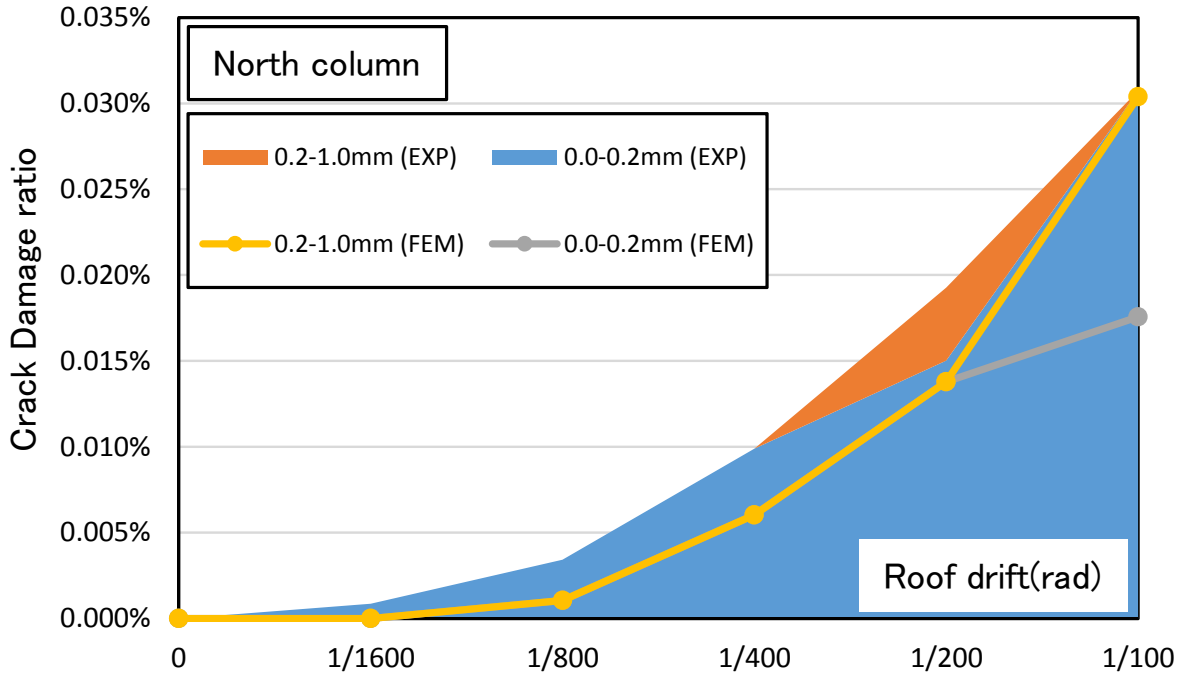

Figure 8. Comparison of experimental and computational variations of crack area damage ratio (North column)

4. DESIGN PHYLOSOPHY FOR RESILIENCY

Damage reduction may be achieved by strengthening the whole structure by properly providing reinforced concrete walls. Strength enhancement with ductile detailed walls may be an easy and economical solution. Another way of damage reduction is low damage structural systems such as self-centering rocking walls. Self-centering rocking wall is a ductile system which suffers very little structural damage since deformation of structures concentrates on interfaces between structural components. With these two extreme systems (strong system and ductile system), designers may choose a preferred low damage structural system among strong systems, ductile systems, or system in-between to achieve much smaller damage level. All these systems are termed low damage system in a broader sense and play an important role to achieve resiliency. Design philosophy of strength-based concept and conventional ductile moment resisting frame concept is shown in Figure 9 (Fukuyama et al. 2015). This paper especially describes the effort of crack evaluation of strength-based reinforced concrete frame since this is one of unique research efforts on resilient reinforced concrete structures in Japan. Crack simulation under seismic loading has been conducted by several researchers in Japan (Maeda et al. 2004, Sato and Naganuma 2011). Their experimental work dealt with scaled model beams and columns and their simulation model has not been validated with real scale building members.

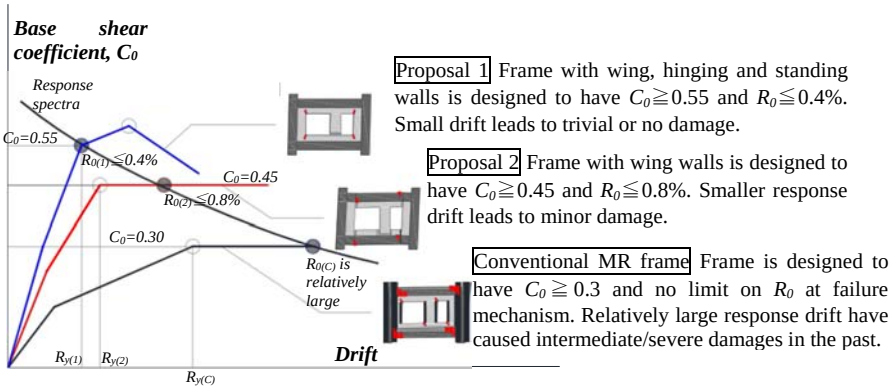

Figure 9. Design philosophy of reinforced concrete buildings for less damage (Fukuyama et al. 2015)

5. CONCLUSIONS

In order to assess damage state, complete residual flexural crack profiles (crack spacing, width, and length) were simulated for the real scale five story reinforced concrete building specimen tested in 2014.

- Accumulated crack width show that crack width and spacing were well simulated for peak points of each cycles.
- Crack length can be simulated by making two assumptions; concrete does not deform, and crack is invisible if crack width is less than the limit crack width.
- Computed crack area damage ratio simulated experimental results relatively well. Computed results should be improved for beams and walls.

The authors hope that simulation of complete crack profiles improves damage evaluation for serviceability and reparability limit states.

6. ACKNOWLEDGMENTS

This study was carried out by a joint study of National Technology Development Project of MLIT “Development of function sustaining technologies for buildings used as Disaster Prevention Bases” (2013～ 2016) and Priority Research Program of BRI Development on Seismic Design Method for Building with Post Earthquake Functional Use”(2013～2015). The efforts in measuring concrete cracking by Tokyo Institute of technology, Tokyo University of Science and Tohoku University and seven participating companies are gratefully acknowledged. A part of this study was conducted as Scientific Research A (PI: Susumu Kono) of JSPS Grant-in-Aid program. Some financial support was also granted by the World Research Hub Initiative of the Institute of Innovative Research and the Collaborative Research Project of Materials and Structures Laboratory at Tokyo Institute of Technology.

7. REFERENCES

Architectural Institute of Japan, Guidelines for Performance Evaluation of Earthquake Resistant Reinforced Concrete Buildings (Draft), 2004.

CEB-FIP: Model Code for Concrete Structures, 15.2.3 Limit states of cracking, pp.156-160, 1978

Ciampi, V. et al.: Analytical Model for Concrete Anchorages of Reinforcing Bars Under Generalized Excitations, *Report No. UCB/EERC-82/23*, Univ. of California, Berkeley, Nov., 1982

Fukuyama, H.: Static Loading Test on A Full Scale Five Story Reinforced Concrete Building utilizing Wing Walls for Damage Reduction, *Summaries of technical papers of Annual Meeting Architectural Institute of Japan*. C-2, 2015, pp. 361-362.

ITOCHU Techno Solutions Corporation: Science and Engineering Systems Division: *Final user's manual*, 2016

Izumo J., Shima H., and Okamura H.: Analytical Model for Reinforced Concrete Panel Elements Subjected to In-Plane Forces, *Concrete Research and Technology*, Vol. 25 (1987), No. 9, Pp. 107-120

JBDPA (The Japan Building Disaster Prevention Association), *Seismic Evaluation and Retrofit*, 2015

Kabeyasawa T., Mukai T., Fukuyama H., et al.: A Full Scale Static Loading Test on Five Story Reinforced Concrete Building Utilizing Columns with Wing Walls, *Journal of Structural and Construction Engineering*, Transactions of AIJ, Vol. 81, 2016, No. 720, 313-322.

Kabeyasawa T., Mukai T., Fukuyama H., Suwada H., and Kato H.: Full-scale static loading test on a five story reinforced concrete building, *16th World Conference on Earthquake Engineering*, Santiago Chile, January 9 – 13, 2017, Paper No. 1242

Kitamura F.: Damage evaluation of five-story building by nonlinear finite element analysis, *Master thesis of Tokyo Instute of Technology*, 2017.

Kono S., Kitamura F., Yuniarsyia E., Watanabe H., Mukai T., Mukai D.: Efforts to develop resilient reinforced concrete building structures in Japan, *Proceedings of the Fourth Conference on Smart Monitoring, Assessment and Rehabilitation of Civil Structures*, Sept 13-15, 2017, Zurich, Switzerland, Paper ID #KN30, 2017.

Ministry of Land, Infrastructure, Transportation and Tourism (MLIT): *The 2015 guidelines of structural design technology of buildings*, 2015.

Naganuma K.: Stress – strain relationship for concrete under triaxial compression, Journal of Structural and Construction Engineering, *Transactions of AIJ*, 1995, No. 474, pp. 163-170.

Sato Y. and Naganuma K.: Crack Width Analysis Using Smeared-Crack-Based FEM: Part 8, *Summaries of tech. papers of Annual Meeting Architectural Inst. of Japan*. C-2, 2011, pp. 241-242.

Maeda M., Nakano Y., and Lee K.: Post-Earthquake Damage Evaluation for R/C Buildings based on Residual Seismic Capacity. *Proc. of 13 World Conference on Earthquake Engineering*, (2004), 1179-